A SEMI-EXPLICIT, VARIABLE-STEPSIZE, TIME-REVERSIBLE INTEGRATOR FOR CONSTRAINED DYNAMICS

ERIC BARTH[†], BENEDICT LEIMKUHLER[‡] AND SEBASTIAN REICH[§]

Abstract. This article describes the design and implementation of a variable timestep method for simulating time-reversible constrained dynamical systems. Based on the Adaptive Verlet method of Huang and Leimkuhler [14], and the SHAKE [23] and RATTLE [1] discretizations, the new method (VRATTLE) defines a mapping of the constraint manifold which preserves the reversible structure. It achieves this through the solution of a single additional scalar nonlinear equation at each timestep, together with the equations of constraint. As a nontrivial application, we simulate the dynamics of an elastic (inextensible, unshearable) rod undergoing large deformations and collisions with the sides of a bounding box. Numerical experiments indicate that adapting the stepsize using VRATTLE can smooth the numerical energy and improve the overall efficiency of the simulation.

Key words. symplectic methods, time-reversible methods, adaptive timestepping, variable stepsize methods, nonlinear elastic dynamics, rod models, holonomically constrained Hamiltonian systems, Verlet, leapfrog, SHAKE, RATTLE

AMS(MOS) subject classifications. 65L05, 70-08, 70F20

1. Introduction and Background. This article proposes an improved integration method for constrained dynamics problems such as arise in molecular and mechanical applications. The discretization scheme can be viewed as providing a time-reversible approach to varying the stepsize. We show how to implement the method efficiently compared to standard fixed-stepsize constrained discretizations (SHAKE/RATTLE) and discuss the choice of a time reparameterization function. As a nontrivial application for the new scheme, we compute the dynamics of an elastic rod subject to impact with an obstacle (a bounding box).

While mechanical models continue to develop in both accuracy and complexity, the methods used for propagation in time have remained remarkably unchanged, consisting generally of either fixed timestep integration with a simple scheme such as Verlet (leapfrog) or implicit midpoint, or else variable timestepping with a standard off-the-shelf ODE solving routine. With some exceptions (see [15] for a survey in the context of molecular modeling), there have been few successful efforts to meddle with the standard integration framework. Several authors have noted that traditional adaptive techniques for varying the timestep are unsuitable for Verlet [24], and other symplectic schemes [8]. Yet many inefficiencies are caused by the use of simplistic schemes, and a great deal of work on fast evaluation of force fields in molecular dynamics and computation of spatial derivatives in elasticity is wasted as this key element (which determines the total number of force evaluations) is neglected. This article discusses advanced timestepping schemes for constrained dynamics problems which are both (1) faithful to symmetries of the problem and (2) frugal in the computation of the applied force

[†] Howard Hughes Medical Institute and Courant Institute of Mathematical Sciences, New York University New York, NY 10012, U.S.A. (barthe@cims.nyu.edu).

[‡] Department of Mathematics, the University of Kansas, Lawrence, KS 66045, U.S.A. (leimkuhl@math.ukans.edu). Supported by NSF grant no. DMS-9303223.

[§] ZIB Konrad-Zuse-Zentrum, Takustr. 7, 14195 Berlin (reich@zib.de).

field.

An example of a conservative elastic dynamics problem is the model of an inextensible, unshearable Cosserat rod as described by Antman [2] and recently treated by Maddocks and Dichmann [9]. After spatial discretization, the equations of motion can be viewed as a collection of constrained rigid body motions. The forces are computed from a discretized interaction potential. The rod model has several potential biological applications [17, 19].

For mechanical systems such as the rod, several authors (see [9, 10, 27]) have proposed the use of implicit integration methods. These methods solve the ODE equations after method-of-lines or other spatial discretization using schemes such as the symplectic-reversible implicit midpoint method (see [9]) or a time-reversible energy-momentum integrator (see [10]). In general, several evaluations of both the force and constraint functions, as well as their derivatives are needed at each timestep. The implicit methods typically treat all forces and variables uniformly — despite the very different natures and roles of positions, momenta, and various multipliers. In the case of the impetus-striction scheme of [9] which enables the treatment of constraints, the complexity of the associated vector field is substantially increased and there is a possibility of drift from the constraint manifold. If such a model were to incorporate long-range interaction potentials (e.g. due to charges placed on the rod), the computational costs would be still greater.

Compared with explicit or semi-explicit schemes such as leapfrog, implicit schemes sometimes allow larger timesteps to be used, but they generally sacrifice some accuracy in the highest frequency components. While for linear models the high frequency modes can be decoupled from the slow modes (which are typically of greater interest) the strong interactions between modes in nonlinear problems may lead to nonlinear instabilities (e.g. resonances) in large timestep simulations. A discussion of resonances in simple molecular models treated with an implicit integrator was given in [18]. Experiments with a careful implementation of a nonlinear implicit method combining aspects of linearization dynamics and the implicit midpoint method have indicated that efficiency improvements are occasionally possible from implicit methods in molecular simulation [5], however it was observed in that work that for large timesteps, multiple solutions of the nonlinear equations can destabilize the time integration. Experience with molecular models and with other complex physical systems seems to suggest the desirability of methods requiring only *one force evaluation per timestep*. For this reason, we favor the use of *semi-explicit* methods. Such schemes may require the solution of one or several algebraic equations (e.g. to satisfy constraint relations), but they only require a single applied force computation at each timestep.

Regardless of whether one uses an implicit, explicit, or semi-explicit method, variable stepsizes are needed for two reasons: (1) very strong local applied forces present in the system (e.g. collisions), and (2) large internal (constraint) forces due to occasional events such as when a rod or joint is subject to a high tension. The latter type of problem may occur in constrained systems, regardless of the presence

or strength of applied forces, and would be reflected in the form of large local Lagrange multipliers along the trajectory. Our view is that when forces of either type strengthen during simulation, the stepsize must be reduced appropriately in order to maintain the stability and accuracy of the numerical method.

1.1. Time Transformations. To improve the numerical integration of N-body coulombic systems, various authors have applied time transformations [6, 28] of the extended phase space. Starting from the phase space Hamiltonian $H = H(p, q)$, they construct a new Hamiltonian $\tilde{H}$ by the *Poincaré transformation*

$$\tilde{H} = (H - \gamma)/U,$$

with U a positive, scalar-valued differentiable function of positions and momenta, and γ representing a new variable canonically conjugate to time. Hamilton's equations are then

$$\begin{aligned}
\frac{dq}{d\tau} &= \frac{1}{U}\nabla_p H + (H-\gamma)\nabla_p(\frac{1}{U}),\\
\frac{d\gamma}{d\tau} &= 0,\\
\frac{dp}{d\tau} &= -\frac{1}{U}\nabla_q H - (H-\gamma)\nabla_q(\frac{1}{U}),\\
\frac{dt}{d\tau} &= \frac{1}{U}.
\end{aligned}$$

Here τ represents a "fictive time."

These Hamiltonian equations can be integrated using a symplectic discretization scheme. This idea has been explored recently by Reich[22] and Hairer [12]. Although it is possible to obtain a first order explicit symplectic method for the extended phase space Hamiltonian, proposed higher-order methods appear to require the work of several force evaluations per timestep, a serious drawback for large computations.

Instead of treating the extended phase space Hamiltonian system directly, we propose to simplify the equations along the energy surface. For given initial $q(0) = q_0$ and $p(0) = p_0$ and $\gamma \equiv \gamma(0) = H(q_0, p_0)$, the terms involving derivatives of $\frac{1}{U}$ drop out and we obtain* (along this trajectory)

$$\frac{dq}{d\tau} = \frac{1}{U}\nabla_p H, \tag{1.1}$$

$$\frac{dp}{d\tau} = -\frac{1}{U}\nabla_q H, \tag{1.2}$$

$$\frac{dt}{d\tau} = \frac{1}{U}. \tag{1.3}$$

The solution of (1.1)–(1.3) passing through $(q(0), p(0)) = (q_0, p_0)$ is thus also the solution of a certain Hamiltonian system. Fixed steps of size h in τ translate into variable timesteps of size roughly h/U in t; if U is chosen appropriately, many more timesteps will be taken at difficult points along the integration.

* Time transformations of this type were introduced by Sundman in early theoretical work on the stability of solutions of the 3-body problem [26].

Although it is important to recognize that (1.1)–(1.3) does *not* itself constitute a Hamiltonian system, (1.1)–(1.3) does possess a time-reversal symmetry, i.e.

$$\mathcal{R} \circ \phi_\tau \circ \mathcal{R} = \phi_{-\tau},$$

where $\mathcal{R}$ is the mapping of phase-space that takes (q,p) to $(q,-p)$, and ϕ_τ is the time τ flow map of the system (i.e. the mapping which takes a given point of phase space to its evolution through τ units of time). Following recent developments [25, 7, 13], we believe that the time-reversal symmetry is important for accurate long term integration.

1.2. Unconstrained Methods. Results given in [14] support the use of a time-reversible variable stepsize approach for unconstrained N-body systems. In [14], a symmetric numerical method for integrating (1.1)–(1.3) was proposed based on the Verlet/leapfrog method. This scheme was explicit in its use of the force, time-reversible, and second order. There are in fact a number of different reversible one-step methods which could be used for integrating the reparameterized problem. To narrow the discussion, we divide these methods into three categories:

I. Explicit methods.

II. Methods explicit in q but implicit in p.

III. Implicit methods.

In this article, we primarily concern ourselves with methods of type I and II. Methods of category II do not require multiple force evaluations (or similar added computational work) in a timestep, although they may require multiple calculations of, e.g., the product of the mass matrix and the momentum. As we anticipate applying these methods to problems in which the force evaluations represent the primary work, we believe that methods of types I and II are equally of interest.

The Adaptive Verlet method of [14] can be written in the form:

$$q_{n+1} = q_n + \frac{h}{\rho_{n+\frac{1}{2}}} p_{n+\frac{1}{2}}, \tag{1.4}$$

$$p_{n+\frac{1}{2}} = p_{n-\frac{1}{2}} - \frac{h}{2}\left(\frac{1}{\rho_{n-\frac{1}{2}}} + \frac{1}{\rho_{n+\frac{1}{2}}}\right)\nabla V(q_n), \tag{1.5}$$

$$\rho_{n+1/2} + \rho_{n-1/2} = U(q_n, p_{n-\frac{1}{2}}) + U(q_n, p_{n+\frac{1}{2}}). \tag{1.6}$$

We will reformulate this method in order to illuminate its properties and suggest variations of the basic scheme. First, introduce the following expressions for p at the timesteps and q at half steps:

$$p_{n+1} = p_{n+\frac{1}{2}} - \frac{h}{2\rho_{n+\frac{1}{2}}}\nabla V(q_{n+1}),$$

$$q_{n+\frac{1}{2}} = q_n + \frac{h}{2\rho_{n+\frac{1}{2}}} p_{n+\frac{1}{2}}.$$

Next shift the discretization by a half-step (replacing e.g. q_n by $q_{n+\frac{1}{2}}$, etc.) to obtain the new formulation

$$q_{n+\frac{1}{2}} = q_n + \frac{h}{2\rho_n} p_n, \tag{1.7}$$

$$p_{n+\frac{1}{2}} = p_n - \frac{h}{2\rho_n}\nabla V(q_{n+\frac{1}{2}}), \tag{1.8}$$

$$\rho_{n+1} + \rho_n = U(q_{n+\frac{1}{2}}, p_n) + U(q_{n+\frac{1}{2}}, p_{n+1}), \tag{1.9}$$

$$q_{n+1} = q_{n+\frac{1}{2}} + \frac{h}{2\rho_{n+1}}p_{n+1}, \tag{1.10}$$

$$p_{n+1} = p_{n+\frac{1}{2}} - \frac{h}{2\rho_{n+1}}\nabla V(q_{n+\frac{1}{2}}). \tag{1.11}$$

In this formulation, the reversible structure becomes clear. The mapping $\hat{\phi}_h$ defined by equations (1.7–1.11),

$$\begin{pmatrix} q_{n+1} \\ p_{n+1} \\ \rho_{n+1} \end{pmatrix} = \hat{\phi}_h \begin{pmatrix} q_n \\ p_n \\ \rho_n \end{pmatrix},$$

respects the symmetry $p \to -p$, $q \to q$ and $\rho \to \rho$, $h \to -h$. In other words, if the equations defining the step are written as

$$\Psi(q_n, q_{n+1}, p_n, p_{n+1}, \rho_n, \rho_{n+1}; h) = 0,$$

then

$$\Psi(q_n, q_{n+1}, p_n, p_{n+1}, \rho_n, \rho_{n+1}; h) = 0$$

if and only if

$$\Psi(q_{n+1}, q_n, -p_{n+1}, -p_n, \rho_{n+1}, \rho_n; -h) = 0.$$

The Adaptive Verlet method is a type II method. The first two equations (1.7)–(1.8) define the half-step positions and momenta in a completely explicit way, equations (1.9) and (1.11) are then solved simultaneously by substituting the right hand side of (1.11) into the right hand side of (1.9), then solving the resulting equation for ρ_{n+1}. The solution of this equation will involve the recalculation of U for different values of p. Finally the computed value ρ_{n+1} is inserted in (1.10)–(1.11) together with other known quantities to complete the step. Moreover, in the case that the control function U is a function of q only, which is reasonable choice in certain problems, then one observes that the method becomes fully explicit (i.e. of type I).

Examining the form of the method (1.7)–(1.11), a fully explicit method is suggested. We could replace the equation (1.9) by

$$\rho_{n+1} + \rho_n = 2U(q_{n+\frac{1}{2}}, p_{n+\frac{1}{2}}).$$

A fully explicit version of the original formulation (1.4)–(1.6) is also possible. The modified update becomes

$$\rho_{n+1/2} + \rho_{n-1/2} = 2U(q_n, p_n),$$

with p_n calculated according to the equation

$$p_n = p_{n-1/2} + \frac{h}{2\rho_{n-1/2}}\nabla V(q_n).$$

In both cases, there is no longer a scalar nonlinear equation to solve. However, with the addition of constraints, we shall need to solve nonlinear equations anyway at each timestep, and the practical difference between methods of type I and type II is likely to be slight.

An example of a type III method would be to use, in place of (1.9), the equation

$$\rho_{n+1} + \rho_n = U(q_{n+1}, p_{n+1}) + U(q_n, p_n). \tag{1.12}$$

It might appear that this method is also of type II, since the first two equations (1.7)–(1.8) are still explicit, and no new evaluations of ∇V will be required in the simultaneous solution of (1.12), (1.10)–(1.11). However, the solution of the latter equations will require the computation of U for varying values of q. In typical practical cases, the function U monitors the applied force (and perhaps other things as well), so the cost of a reevaluation of U is essentially the same as a force evaluation and we conclude that the method using (1.12) is a type III scheme. Although the type III schemes are typically more expensive to use than either the type I or type II methods, there are situations where their use could be warranted, for example if the stepsize is controlled based on certain easily computed observable quantities and is much cheaper to evaluate than the force itself.

The type I and type II schemes are susceptible to a phenomenon which we call *wobble*. This step-to-step oscillation of the variable ρ arises in those situations where the control function becomes very large, i.e. in the vicinity of collisions. It occurs in explicit methods because of the time lag between evaluations of U (and consequent updates of ρ) and the evaluation of the next timestep. The wobble can be ameliorated by choosing the initial parameter ρ_0 correctly, for example, when using the original Adaptive Verlet method with a step control U based on q only, we set

$$\rho_{-1} = U(q_{-1}).$$

Here, q_{-1} is found by stepping backwards in time from q_0 with timestep $-h$ using equations (1.7)–(1.9) and solving a nonlinear equation. Alternatively, we have also been successful by taking one or two steps forward in time, and approximating $U(q_{-1})$ by extrapolation. In either case, we then put

$$\rho_{-1/2} = \frac{U(q_{-1}) + U(q_0)}{2}.$$

We will discuss the wobble in more detail in §5.

In §2, we generalize the Adaptive Verlet scheme (1.7)–(1.11) to constrained Hamiltonian systems using the SHAKE discretization [23] (or its RATTLE variant [1]), resulting in a system of nonlinear equations which must be solved at each timestep. Although the traditional iterative scheme of [23] can be employed for this purpose, we propose instead to use the symmetric approximate Newton method of [3]. In §3, we describe an efficient implementation of this method. In §4, we use the example of the double pendulum to suggest a choice for the time reparameterization U in the case of the constrained system in which the constraints are subject to substantial strain. In §5 we consider the example of a constrained model of an elastic rod striking an obstacle with a Lennard-Jones type repulsion,

and present numerical experiments which show that the energy error in the numerical solution can be effectively and efficiently "leveled out" by use of the adaptive method. We also consider the treatment of wobble as it arises in this problem.

2. Constrained Hamiltonian Systems and the VRATTLE Method. Time reparameterizations can be introduced in holonomically constrained systems in a precisely analogous way to the unconstrained case. Suppose we have m independent constraining relations $g_i(q) = 0$, $i = 1, \ldots, m$, or, compactly, $g(q) = 0$, where $g = (g_1, g_2, \ldots, g_m)^T$. We introduce a vector of multipliers $\lambda = (\lambda_1, \lambda_2, \ldots, \lambda_m)^T$ and consider a constrained mechanical Hamiltonian of the form $H = \frac{p^T M^{-1} p}{2} + V(q) + g(q)^T \lambda$. The dynamical system is described by

$$\dot{q} = M^{-1} p, \tag{2.13}$$

$$\dot{p} = -\nabla V(q) - g'(q)^T \lambda, \tag{2.14}$$

$$0 = g(q). \tag{2.15}$$

The phase space is the manifold $S = \{(q,p) \in \mathbf{R}^{2N} | g(q) = 0, g'(q) M^{-1} p = 0\}$. Note that the phase space admits the symmetry $p \to -p$. The flow map ϕ_t is here a mapping of S which satisfies $\mathcal{R} \circ \phi_t \circ \mathcal{R} = \phi_{-t}$. The constrained equations of motion can be solved using the RATTLE discretization [1]:

$$q_{n+1} = q_n + h M^{-1} p_{n+1/2}, \tag{2.16}$$

$$p_{n+\frac{1}{2}} = p_{n-\frac{1}{2}} - h \left(\nabla V(q_n) + g'(q_n)^T \lambda_n \right), \tag{2.17}$$

$$0 = g(q_{n+1}). \tag{2.18}$$

and

$$p_n = p_{n-\frac{1}{2}} - \frac{h}{2} \left(\nabla V(q_n) + g'(q_n)^T \mu_n \right), \tag{2.19}$$

$$0 = g'(q_n) M^{-1} p_n. \tag{2.20}$$

Note that (2.19)–(2.20) could be omitted giving rise to the SHAKE discretization [23]. These methods are identical with respect to the propagation of the variable $(q_n, p_{n-1/2})$. In the discussion which follows, we extend the RATTLE discretization to treat the reparameterized equations; SHAKE treatment would be similar.

After introduction of a time reparameterization $dt = \frac{1}{\rho} d\tau$, we obtain the constrained system:

$$\dot{q} = \frac{1}{\rho} M^{-1} p, \tag{2.21}$$

$$\dot{p} = -\frac{1}{\rho} \left(\nabla V(q) + g'(q)^T \lambda \right), \tag{2.22}$$

$$0 = g(q). \tag{2.23}$$

We propose to discretize this using a modification of RATTLE which is naturally suggested by

the semi-explicit adaptive Verlet method (1.4)–(1.6):

$$q_{n+1} = q_n + \frac{h}{\rho_{n+\frac{1}{2}}} M^{-1} p_{n+\frac{1}{2}}, \tag{2.24}$$

$$p_{n+\frac{1}{2}} = p_{n-\frac{1}{2}} - \frac{h}{2}\left(\frac{1}{\rho_{n-\frac{1}{2}}} + \frac{1}{\rho_{n+\frac{1}{2}}}\right)\left(\nabla V(q_n) + g'(q_n)^T \lambda_n\right), \tag{2.25}$$

$$0 = g(q_{n+1}), \tag{2.26}$$

and

$$p_n = p_{n-\frac{1}{2}} - \frac{h}{2\rho_{n+\frac{1}{2}}}\left(\nabla V(q_n) + g'(q_n)^T \mu_n\right), \tag{2.27}$$

$$0 = g'(q_n) M^{-1} p_n, \tag{2.28}$$

$$\rho_{n+\frac{1}{2}} + \rho_{n-\frac{1}{2}} = U(q_n, p_{n+\frac{1}{2}}) + U(q_n, p_{n-\frac{1}{2}}). \tag{2.29}$$

We call the above described method VRATTLE. Note that, similar to RATTLE, (2.27)–(2.28) is not needed for the propagation of the variable $(q_n, p_{n-1/2})$. We call the resulting method VSHAKE.

As for the semi-explicit adaptive Verlet method (1.4)–(1.6), one could replace the ρ-update (2.29) by the explicit formulation

$$\rho_{n+\frac{1}{2}} + \rho_{n-\frac{1}{2}} = 2U(q_n, p_n).$$

VRATTLE is a symmetric one-step method when viewed as a map

$$\hat{\phi}_h : \begin{pmatrix} q_{n-\frac{1}{2}} \\ p_{n-\frac{1}{2}} \\ \rho_{n-\frac{1}{2}} \end{pmatrix} \to \begin{pmatrix} q_{n+\frac{1}{2}} \\ p_{n+\frac{1}{2}} \\ \rho_{n+\frac{1}{2}} \end{pmatrix}.$$

It is possible to construct the method in the time-shifted formulation of Section 1.2, so that $\hat{\phi}$ maps the whole-steps. We will not present the details here, but rather devote the remainder of this paper to discussing the efficient implementation of the scheme (2.24)–(2.29). We consider the selection of a reparameterization function U appropriate for constrained systems, and examine the behavior of several variants in a practical case.

3. Implementation. For the SHAKE/RATTLE discretization, equations (2.16)–(2.18) are combined, resulting in the system of nonlinear equations

$$0 = \mathcal{G}(\lambda_n) = g\left(q_n + hM^{-1}\left(p_{n-1/2} - \frac{h}{2}\left(\nabla V(q_n) + g'(q_n)^T \lambda_n\right)\right)\right).$$

We can solve for the vector of Lagrange multipliers λ_n using Newton's method:

$$\lambda_n^{(k+1)} = \lambda_n^{(k)} - \left(\frac{\partial \mathcal{G}}{\partial \lambda_n}\right)^{-1} \mathcal{G}(\lambda_n^{(k)}). \tag{3.30}$$

Observe that

$$\frac{\partial \mathcal{G}}{\partial \lambda_n} = \frac{h^2}{2} g'(q_*) M^{-1} g'(q_n)^T,$$

where $q_* = q_n + hM^{-1}(p_{n-1/2} + \frac{h}{2}(\nabla V(q_n) + g'(q_n)^T \lambda_n^{(k)}))$. Efficient SOR/Newton methods for solving the linear equations (3.30) were studied in [3].

Now, turning to the new method, equations (2.24)–(2.26) and (2.29) can be combined to give the system of nonlinear equations

$$0 = \mathcal{G}(\rho_{n+1/2}, \lambda_n) \tag{3.31}$$

$$\equiv g\left(q_n + \frac{h}{\rho_{n+1/2}} M^{-1}\left(p_n - \frac{h}{2\rho_{n+1/2}}\left(\nabla V(q_n) + g'(q_n)^T\lambda_n\right)\right)\right) \tag{3.32}$$

$$0 = \mathcal{F}(\rho_{n+1/2}, \lambda_n) \tag{3.33}$$

$$\equiv \rho_{n+1/2} + \rho_n - U(q_n, p_{n+1/2}) - U(q_n, p_n). \tag{3.34}$$

As before, we solve these equations with Newton's method:

$$\begin{bmatrix} \lambda_n \\ \rho_{n+1/2} \end{bmatrix}^{(k+1)} = \begin{bmatrix} \lambda_n \\ \rho_{n+1/2} \end{bmatrix}^{(k)} - \begin{bmatrix} \frac{\partial \mathcal{G}}{\partial \lambda_n} & \frac{\partial \mathcal{G}}{\partial \rho_{n+1/2}} \\ \frac{\partial \mathcal{F}}{\partial \lambda_n} & \frac{\partial \mathcal{F}}{\partial \rho_{n+1/2}} \end{bmatrix}^{-1} \begin{bmatrix} \mathcal{G}(\rho^{(k)}_{n+1/2}, \lambda^{(k)}_n) \\ \mathcal{F}(\rho^{(k)}_{n+1/2}, \lambda^{(k)}_n) \end{bmatrix}. \tag{3.35}$$

For a general step control function $U(q,p)$, we can write the required partial derivatives as:

$$\frac{\partial \mathcal{G}}{\partial \lambda_n} = -\frac{h^2}{2\rho^{(k)}_{n+1/2}} g'(q_*) M^{-1} g'(q_n)^T \lambda_n \tag{3.36}$$

$$\frac{\partial \mathcal{G}}{\partial \rho_{n+1/2}} = -\frac{h}{(\rho^{(k)}_{n+1/2})^2} g'(q_*) M^{-1}\left(p^{(k)}_{n+1/2} - \frac{h}{2\rho^{(k)}_{n+1/2}}\left(\nabla V(q_n) + g'(q_n)^T\lambda_n\right)\right) \tag{3.37}$$

$$\frac{\partial \mathcal{F}}{\partial \lambda_n} = -\frac{\partial U}{\partial \lambda_n} \tag{3.38}$$

$$= -\frac{\partial U}{\partial p_{n+1/2}} \frac{\partial p_{n+1/2}}{\partial \lambda_n} \tag{3.39}$$

$$= -\frac{h}{2\rho^{(k)}_{n+1/2}} \frac{\partial U}{\partial p_{n+1/2}} g'(q_n)^T \tag{3.40}$$

$$\frac{\partial \mathcal{F}}{\partial \rho_{n+1/2}} = 1 - \frac{\partial U}{\partial \rho_{n+1/2}} \tag{3.41}$$

$$= 1 - \frac{\partial U}{\partial p_{n+1/2}} \frac{\partial p_{n+1/2}}{\partial \rho_{n+1/2}} \tag{3.42}$$

$$= 1 + \frac{1}{\rho_{n+1/2}} \frac{\partial U}{\partial p_{n+1/2}} (p_{n+1/2} - p_n). \tag{3.43}$$

The linear equations can be treated with the same techniques as (3.30). Defining $\lambda^{(k+1)}_n = \lambda^{(k)}_n + \Delta\lambda^{(k)}_n$, and $\rho^{(k+1)}_{n+1/2} = \rho^{(k)}_{n+1/2} + \Delta\rho^{(k)}_{n+1/2}$ we have

$$\Delta\rho^{(k)}_{n+1/2} = \left(\frac{\partial \mathcal{F}}{\partial \rho_{n+1/2}} - \frac{\partial \mathcal{F}}{\partial \lambda_n}^T \frac{\partial \mathcal{G}}{\partial \lambda_n}^{-1} \frac{\partial \mathcal{G}}{\partial \rho_{n+1/2}}\right) / \left(-\mathcal{F}(\rho^{(k)}_{n+1/2}, \lambda^{(k)}_n) + \frac{\partial \mathcal{F}}{\partial \lambda_n}^T \frac{\partial \mathcal{G}}{\partial \lambda_n}^{-1} \mathcal{G}(\rho^{(k)}_{n+1/2}, \lambda^{(k)}_n)\right)$$

$$\Delta\lambda^{(k)}_n = -\frac{\partial \mathcal{G}}{\partial \lambda_n}^{-1} \mathcal{G}(\rho^{(k)}_{n+1/2}, \lambda^{(k)}_n) - \Delta\rho_{n+1/2} \frac{\partial \mathcal{G}}{\partial \lambda_n}^{-1} \frac{\partial \mathcal{G}}{\partial \rho_{n+1/2}}.$$

In the equations above, the inverse of the Jacobian matrix $\partial\mathcal{G}/\partial\lambda_n$ multiplies two distinct vectors. The matrix-vector product is implemented through matrix factorization and a triangular matrix solve, rather than inversion. After the factorization of $\partial\mathcal{G}/\partial\lambda_n$, two triangular matrix solves are required to determine the Newton iterates $\lambda^{(k+1)}_n$ and $\rho^{(k+1)}_{n+1/2}$. Thus, for a general time reparameterization function $U(q,p)$, the method requires one extra triangular matrix solve per iteration compared with the fixed stepsize method. A variant of the scheme would replace the Jacobian matrix the Newton iteration by a nearby symmetric matrix, see [3].

4. Choice of time reparameterization U. In few degree-of-freedom gravitational problems, it is common to make U a function of q only. For example, with force a function of position only, we might control the stepsize based on the largest acceleration:

$$U = \max\|f_i\|.$$

Notice that Adaptive Verlet is completely explicit in this case, and that implementation does not require derivatives of U with respect to positions, so no smoothness problems would be anticipated. Alternatives to this choice include basing U on the rate of change of arclength along the phase space trajectory, on the maximum rate of change of arclength traversed by any particle in an N-body problem, or on some other observable quantity which monitors the local difficulty in resolving the trajectory.

For constrained systems, the considerations are similar. We still need to take into account the unconstrained (applied) forces acting on the particles, but the system is also subject to constraint (internal) forces. As a first step, one might anticipate that large constraint forces would lead to large momenta, so that it would be enough to control the step based on the momenta (and perhaps the unconstrained forces) alone. To see that this approach can fail, consider the example of a double planar pendulum swinging in gravity, with constrained equations of motion:

$$\begin{aligned}
m_1\dot{x}_1 &= u_1, & \dot{u}_1 &= -x_1\lambda_1 - (x_1 - x_2)\lambda_2,\\
m_1\dot{y}_1 &= v_1, & \dot{v}_1 &= -y_1\lambda_1 - (y_1 - y_2)\lambda_2 - 1,\\
m_2\dot{x}_2 &= u_2, & \dot{u}_2 &= (x_2 - x_1)\lambda_2,\\
m_2\dot{y}_2 &= v_2, & \dot{v}_2 &= (y_2 - y_1)\lambda_2 - 1,
\end{aligned}$$

$$\begin{aligned}
0 &= \frac{1}{2}(x_1^2 + y_1^2) - 1,\\
0 &= \frac{1}{2}\left((x_1 - x_2)^2 + (y_1 - y_2)^2\right) - 1.
\end{aligned}$$

This problem was considered in [14] in the more familiar angle-angle formulation, and the unconstrained (nonseparable) Hamiltonian equations were discretized with the implicit midpoint method using time reparameterization based on the size of the vector field.

We attempted direct integration of the constrained equations, adjusting the timestep based on the size of the unconstrained vector field,

$$U = U_1(q,p) \equiv \sqrt{p^T M^{-2} p + \|f\|^2}. \tag{4.44}$$

The ratio of masses m_1/m_2 was taken to be 1000.

Figure 1b shows the energy error for trajectories computed with the fixed timestep integrator of (2.16)–(2.18) and for VRATTLE with U_1 from (4.44). Step size for RATTLE was chosen as the average timestep from the VRATTLE integration. In this way, the number of function evaluations is equivalent for the two methods. Peaks in the energy, corresponding to cusp-points in the position trajectories shown in Figure 1a, are evident for both methods, although the magnitude of the energy error is much smaller for VRATTLE. The peaks suggest that the step control function U_1 does not

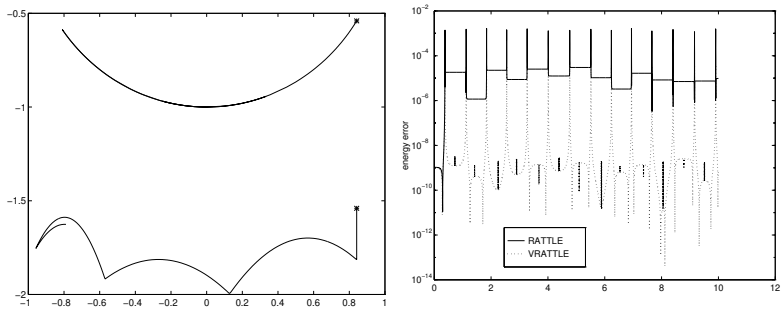

FIG. 1. *(a) Trajectories and (b) Energy error for RATTLE/VRATTLE.*

adequately monitor variation in the integration difficulty. In U_1, we have accounted for kinetic and potential energy, but have neglected the constraint force. Figure 2 shows the magnitude of λ_n (scaled by the square of the timestep), which is proportional to the constraint force, throughout the fixed timestep simulation. Although large multipliers are ultimately reflected in large momenta, the method does not adapt sufficiently rapidly. This simple example indicates that the constraint forces must be considered in the design of an effective step control strategy, at least whenever the constraints are subject to significant strain.

We would like to include the magnitude of the multipliers in the design of U. On the other hand, to be able to apply the VRATTLE method, we must have a step control function U which depends on q and p only. With this in mind, we observe that the equation (2.15) can be differentiated repeatedly with respect to time t using the time derivatives in (2.13),(2.14), obtaining an equation which can be solved for λ, i.e. along solutions,

$$0 = \frac{d}{dt} g(q) = g'(q)\dot{q} = g'(q)M^{-1}p,$$

and

$$0 = \frac{d}{dt} g'(q)M^{-1}p = g''(q)(M^{-1}p, M^{-1}p) + g'(q)M^{-1}(-\nabla V(q) - g'(q)^T\lambda).$$

Here g'' represents the tensor second derivative of the constraint function g. Assuming $g'(q)M^{-1}g'(q)^T$ is nonsingular, we can solve the latter equation for λ as a function of q and p.

Because it is an important practical case, we specialize this computation to the case of quadratic length constraints of the form

$$g(q) = \|q_i - q_j\|^2 - L^2 \equiv \tilde{g}(q) - L^2.$$

We give two lemmas which illuminate the special structure of (2.28):

LEMMA 4.1. *For a single quadratic constraint* $g(q) = 0$ *and* $G = \nabla_q g(q)$,

$$\frac{d^2}{dt^2} g(q) = G(\dot{q})\dot{q} + G(q)\ddot{q}.$$

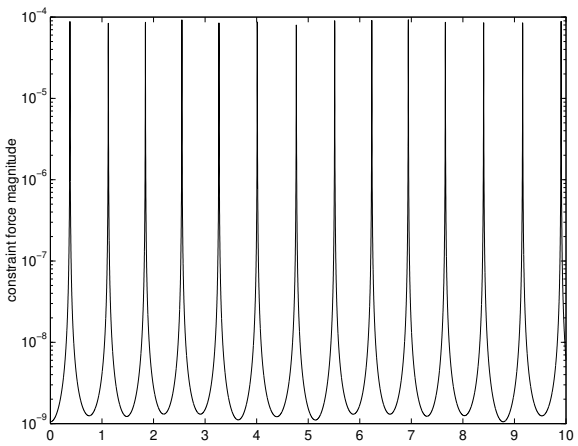

FIG. 2. *Variation of Lagrange multiplier λ_n throughout RATTLE integration.*

LEMMA 4.2. *For any vector r, quadratic constraints written as $g(q) = \frac{1}{2}\tilde{g}(q) - L^2 = 0$, and $G = \nabla_q g(q)$,*

$$G(r)r = \tilde{g}(r).$$

Using 4.1 and the constrained equations of motion (2.22)–(2.23) we have

$$0 = \frac{d^2}{dt^2} g(q), \tag{4.45}$$

$$= G(M^{-1}p)M^{-1}p + G(q)M^{-1}\dot{p}, \tag{4.46}$$

$$= G(M^{-1}p)M^{-1}p + G(q)M^{-1}(f(q) - G^T\lambda). \tag{4.47}$$

We can solve this equation for λ in terms of p and q,

$$\lambda = \Lambda(q,p) \equiv (GM^{-1}G^T)^{-1}\left(G(M^{-1}p)M^{-1}p + G(q)M^{-1}f\right). \tag{4.48}$$

We use the notation $\Lambda(q,p)$ to distinguish the expression in (4.48) from the vector of Lagrange multipliers λ_n we seek to compute at each step of the discretization. In this form it is clear that the computation of λ does not require a great deal of overhead in addition to what would be required in a standard fixed stepsize (SHAKE/RATTLE) integration. The matrix $GM^{-1}G^T$ must be computed and factored anyway if we are using the efficient SNIP (symmetric Newton) iterative scheme of [3] for solving the nonlinear equations.

Although (4.48) could be substituted back into the constrained equations of motion (2.22)–(2.23) to eliminate λ, there are several deficiencies to such an approach; in particular the vector field would be more complex, discretization errors can accumulate which eventually violate the constraint condition (2.23), and symplectic or time-reversal symmetries would be destroyed by standard schemes for the resulting system. Instead, we use (4.48) only for the purpose of step size control.

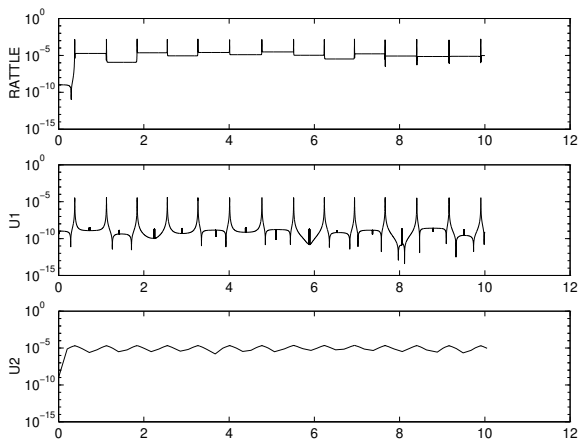

FIG. 3. *Energy error for RATTLE and VRATTLE with step control functions U_1 and U_2.*

To implement the discretization with

$$U_2(q,p) \equiv \|\Lambda(q,p)\|, \tag{4.49}$$

we require the partial derivatives with respect to p. Applying 4.2 to $G(M^{-1}p)M^{-1}p$ and differentiating, we have

$$\frac{\partial U}{\partial p} = \Lambda(q,p)^T (GM^{-1}G^T)^{-1} G(M^{-1}p)M^{-1}.$$

Figure 3 gives energy error for RATTLE, VRATTLE with step control function U_1 and VRATTLE with U_2. The peaks in the energy which were present in the RATTLE and VRATTLE–U_1 simulations are eliminated with VRATTLE–U_2. Figure 4 gives the step size throughout the VRATTLE(A) integrations with the two step control functions. The maximum stepsize with U_2 is several orders of magnitude larger than for U_1. This observation suggests the desirability of limiting stepsize growth. A mechanism for controlling the maximum and minimum stepsize is suggested in [14]. For some step control function R, define

$$\tilde{R} = \frac{R+m}{\frac{1}{M}(R+m)+1} \tag{4.50}$$

where $0 < m \ll M$. In this way bounds

$$m \approx \frac{1}{\frac{1}{M}+\frac{1}{m}} < \tilde{R} < M.$$

are introduced on the step control function and hence on the VRATTLE stepsize.

5. An Elastic Rod Model. We will examine various approaches on a constrained model of an inextensible, unshearable elastic rod for which the applied force arising in a collision determines the proper stepsize. This nontrivial example also demonstrates that a semi-explicit, time-reversible rigid body integrator based on the VRATTLE integrator can provide a sound adaptive framework for conservative multibody integration.

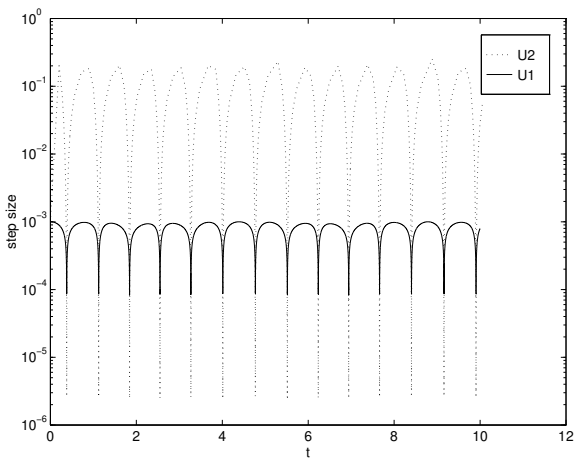

FIG. 4. *Step size for VRATTLE with step control functions U_1 and U_2.*

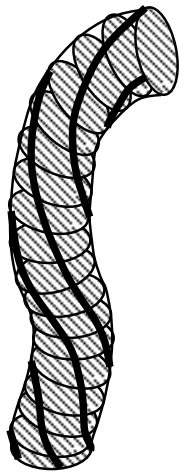

FIG. 5. *A Cosserat rod: dynamics are formulated in terms of rigid body motion of a material cross-section. The superimposed curves indicate twist.*

The Cosserat theory of rods [2] describes the motion of a rod in terms of the dynamics of a material cross section. The dependent variables are vectors z, d_1, d_2, and d_3, all parameterized by arclength. $z = z(s)$ represents the center of mass of the rod cross section at a point s units along the length of the rod. d_1, d_2 and d_3 are an orthonormal system of directors with d_1 and d_2 describing the plane in which the cross section lies and d_3 being oriented along the rod "backbone."

Antman [2] gives the formulae:

$$\frac{\partial d_i}{\partial s} = \vec{u} \times d_i, \qquad i = 1, 2, 3 \tag{5.51}$$

which relate motions in the directors to the strains $\vec{u} = (u_1, u_2, u_3)^t$ associated to bend and twist. The inextensibility and unshearability constraints are expressed by

$$d_3 = \frac{\partial z}{\partial s}.$$

To make explicit the constraints of orthonormality of the system of directors we may write:

$$d_1 \perp d_2,$$
$$|d_1| = |d_2| = 1,$$
$$d_3 = d_1 \times d_2.$$

We wish to write equations of motion in terms of the arclength z and the two cross-sectional directors d_1 and d_2. Specifically, we will express the kinetic energy T in terms of the $\dot{z}$, $\dot{d}_1$ and $\dot{d}_2$, and we can then express the potential energy V of the rod in terms of d_1, d_2, $\frac{\partial d_1}{\partial s}$ and $\frac{\partial d_2}{\partial s}$. The constraints are written as equations involving only d_1, d_2, and z_s. After spatial discretization, we arrive at constrained equations in the form treated in [4].

The kinetic energy can be written in terms of $\dot{z}$, $\dot{d}_1$, $\dot{d}_2$ as

$$\begin{aligned} T &= \frac{1}{2}\int_0^1 \frac{\rho}{3}\left(|\dot{q}_1|^2 + |\dot{q}_2|^2 + |\dot{q}_3|^2\right) ds \\ &= \frac{1}{6}\int_0^1 \rho\left(|\dot{z} + \delta_1\dot{d}_1|^2 + |\dot{z} + \delta_2\dot{d}_2|^2 + |\dot{z} - \delta_1\dot{d}_1 - \delta_2\dot{d}_2|^2\right) ds. \end{aligned}$$

The potential energy of the rod is given in terms of u_1, u_2 and u_3 as

$$V = \frac{1}{2}\int_0^1 \left(K_1 u_1^2 + K_2 u_2^2 + K_3 u_3^2\right) ds.$$

We need to obtain formulas for the components of $\vec{u}$ in terms of the directors. To do this, we use $d_3 = d_1 \times d_2$ and solve the constraining relations (5.51) for u:

$$\begin{aligned} u_1 &= (d_1 \times d_2) \cdot \frac{\partial d_2}{\partial s}, \\ u_2 &= -(d_1 \times d_2) \cdot \frac{\partial d_1}{\partial s}, \\ u_3 &= d_1 \cdot \frac{\partial d_2}{\partial s}. \end{aligned}$$

The six constraints on this system consist of

$$\begin{aligned} g_1 &= d_1 \cdot d_2, \\ g_2 &= d_1 \cdot d_1 - 1, \\ g_3 &= d_2 \cdot d_2 - 1, \\ \begin{bmatrix} g_4 \\ g_5 \\ g_6 \end{bmatrix} &= \frac{\partial z}{\partial s} - d_1 \times d_2. \end{aligned}$$

Letting

$$q = \begin{bmatrix} z \\ d_1 \\ d_2 \end{bmatrix},$$

we define the constrained Lagrangian using our expressions for T, V and g by

$$\mathcal{L} = T(\dot{q}) - V(q) - \int_0^1 g(q)^T \mu ds.$$

From which we obtain the canonical momenta p by the usual variational differentiation:

$$p = \frac{\delta \mathcal{L}}{\delta \dot{q}} = M\dot{q},$$

where M is a constant matrix. After re-expressing the kinetic energy T as a function of the momenta, $T(\dot{q}) = \tilde{T}(p)$, we obtain a constrained Hamiltonian system with Hamiltonian

$$\mathcal{H} = \tilde{T}(p) + V(q) + \int_0^1 g(q)^T \mu ds.$$

A natural discretization of this system is via finite differences in s; this corresponds to replacing the elastic rod by a collection of cross-sectional rigid bodies. In order to obtain second order in the spatial variable, we follow the idea of Maddocks and Dichmann [9] to use values of both q and p at half-steps in Δs but to write equations at the even steps. Specifically, our constrained spatially discretized Hamiltonian is obtained by replacing integration by summation and

$$p(s_i) \to \frac{p_{i-1/2} + p_{i+1/2}}{2},$$

$$q(s_i) \to \frac{q_{i-1/2} + q_{i+1/2}}{2},$$

where the subscripts here index the variables corresponding to successive finite cross-sections. For the inextensibility constraint, we discretize $\frac{\partial z}{\partial s}(s_i)$ by $(z_{i+1/2} - z_{i-1/2})/\Delta s$ and use a similar treatment for the partial derivatives of d_1 and d_2 where they arise in the potential energy function. This results in a constrained mechanical system to which SHAKE/RATTLE (or VSHAKE/VRATTLE) can be applied.

We can use any of our family of nonlinear solvers (the SOR/Newton solvers) to treat the nonlinear equations at each timestep. As described, the potential energy and constraint functions have a nearest neighbor topology which leads to block tridiagonal constraint Jacobian $\frac{\partial \mathcal{G}}{\partial \lambda_n}$ with 6×6 blocks.

As a test problem for the rod model and the new adaptive-timestep time–reversible integrator for constrained systems we consider an elastic rod with one end fixed. The resulting strut is placed inside a box whose walls are modeled by a Lennard-Jones potential, typically encountered in molecular models, which, for the ith cross-sectional center of mass, makes a contribution to the potential energy of the form

$$V_i = \epsilon \left(\left(\frac{\beta}{\Delta_i} \right)^{12} - 2 \left(\frac{\beta}{\Delta_i} \right)^{6} \right).$$

This potential is characterized by a rapidly decaying tail for large separations Δ_i, a steep repulsive wall for small Δ_i, and mildly attractive region at intermediate separations. It can be viewed as a very slightly softened wall. Here ϵ gives the attractive strength and β determines the width of the attractive region. In our simulations we used the values $\epsilon = 0.1$ and $\beta = 0.25$. For this system, unlike the pendulum example from §4 in which large constraint forces required careful treatment, the large systematic forces associated with close rod/wall interactions require small timesteps for correct

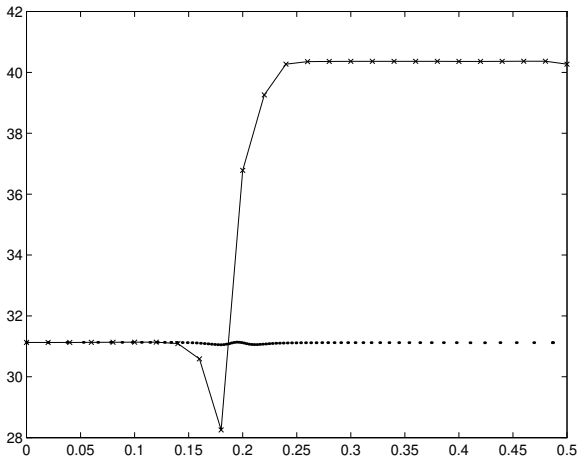

FIG. 6. *Total rod energy along trajectories computed with RATTLE (−×−) and VRATTLE (···) with the same initial stepsize. The rod/wall collision occurs at* $t \approx 0.2$.

resolution of the collisions. In this case it is natural to implement a step control function which monitors some power α of the minimum separation between the rod and the wall,

$$U_3 = \max_i \left(\frac{1}{\Delta_i}\right)^{\alpha}. \tag{5.52}$$

For this choice, no additional nonlinear equations need to be solved since $\rho_{n+1/2}$ is given explicitly by equation (2.29).

From a vertical initial position, the sections of the rod are assigned horizontal velocities consistent with the constraints. Figure 6 shows the total energy of the rod along RATTLE and VRATTLE trajectories computed with the same initial stepsize. The rod/wall collision occurs at $t \approx 0.2$. This figure shows that the VRATTLE scheme can improve the robustness of the integration method by properly reducing stepsize during an event (the collision with the box wall).

For smaller initial stepsize, such that the abrupt energy jump shown in Figure 6 is absent, rapid variation in energy is still present. We show in Figure 7 error behavior for RATTLE and VRATTLE with step control function U_3 and $\alpha = 3.0$. Energy error is given for RATTLE with timestep h=0.0029, and VRATTLE with initial timesteps h_0=0.02 and h_0=0.04. The RATTLE timestep was chosen to integrate over the interval with the same number of steps (and force evaluations) as the variable timestep VRATTLE simulation with h_0=0.02. The maximum energy error for VRATTLE with h_0=0.04 is smaller than that of RATTLE, even though *only half as many steps were required.* Notice in all cases, the energy error due to the collisions would be considerably reduced by the adaptive timestep method compared to the fixed step method with the same *initial* step size.

We also incorporated a standard step control based on normed vector field and were able to control the energy fluctuation. However, better results were typically obtained with step control based on separation from the bounding walls.

The efficiency of VRATTLE with respect to maximum energy error is illustrated in Figure 8. This

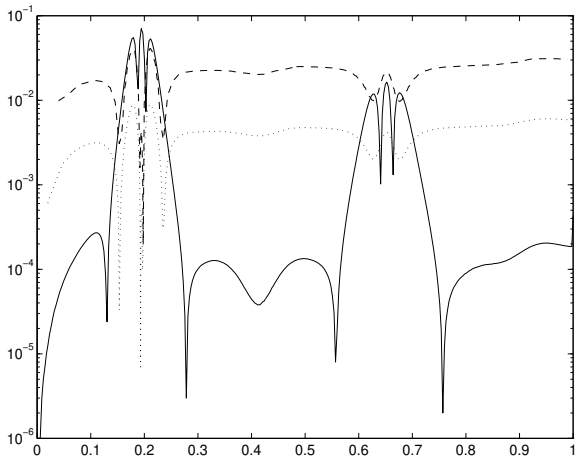

FIG. 7. *Energy error for rod/box collision: RATTLE with stepsize h=0.0029 (—), VRATTLE with initial stepsizes h_0=0.02 (···), and h_0=0.04 (−−). The RATTLE timestep was chosen so as to duplicate the number of steps required by VRATTLE (h_0=0.2) to cover the integration interval. Step control function U_3 is used with $\alpha = 3.0$.*

work-error diagram shows that the adaptive method outperforms the fixed stepsize method at various error tolerances, and that the relative improvement of the adaptive method appears to be greatest with a more severe error tolerance.

6. Stepsize Wobble and A Smoothed Scheme. We next turn to the "wobble" phenomenon mentioned in the introduction. Figure 9 shows the value of the variable $\rho_{n+1/2}$ and the fictive timestep $h/\rho_{n+1/2}$ over the course of a VRATTLE simulation with time reparametrization function eq. (5.52). In the top views, the initial values were taken as $(p, q, \rho) = (p_0, q_0, U(q_0))$. In the middle views, the initialization was done as described in the introduction. It is clear from the figure that, depending on the choice of initial values, ρ can oscillate with substantial amplitude with increasing U, while the amplitude of oscillation in the fictive timestep remains essentially constant (but small).

As an alternative, we implemented the method obtained by replacing equation (1.9) with (1.12) in the constrained adaptive scheme. For the purpose of the remainder of this section, we refer to the VRATTLE method by VRATTLE(A) and the alternative Type III method obtained by using (1.12) as VRATTLE(B).

In implementing this reformulated method, it is important to note that the step control must be differentiable. We propose the smoothed step control function

$$\tilde{U}_3(q) = \left[\sum_{ij} \frac{1}{\Delta_i^\mu} \right]^{\alpha/\mu} . \tag{6.53}$$

This smoothed variant can be viewed as first taking the L_μ norm of the vector with components $1/\Delta_i$, then raising the result to the α power. For large μ, the inverse minimum separation will dominate the sum. We note that the use of the smoothed step control function $\tilde{U}_3$ did not remedy the stepsize

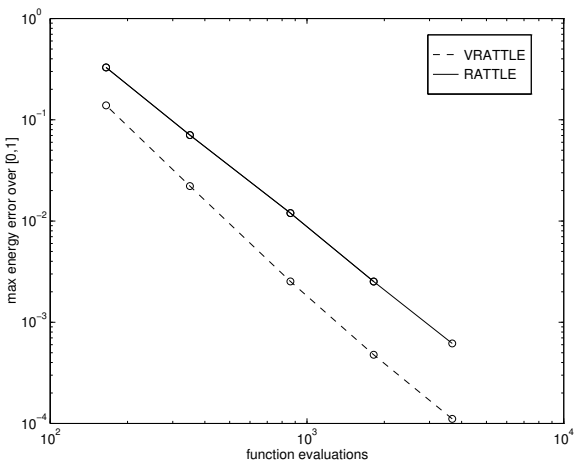

FIG. 8. *Comparison of work-energy diagrams for RATTLE and VRATTLE with step control function* U_3 *(*$\alpha = 3.0$*).*

wobble in VRATTLE(A).

To demonstrate the wobble and possible remedies, Figure 9 gives the value of the time scaling factor $\rho_{n+1/2}$ and fictive timestep for three VRATTLE simulations. The top views correspond to VRATTLE(A) with reparameterization function (eq. (5.52)) initialized with $\rho_0 = U_3(q_0)$. The middle views are for VRATTLE(A)–U_3 with initialization of ρ_0 as described in the introduction. The lower views correspond to VRATTLE(B) simulation with reparameterization function (eq. (6.53)) initialized with with $\rho_0 = \tilde{U}_3(q_0)$. The stepsize wobble is eliminated by the new method.

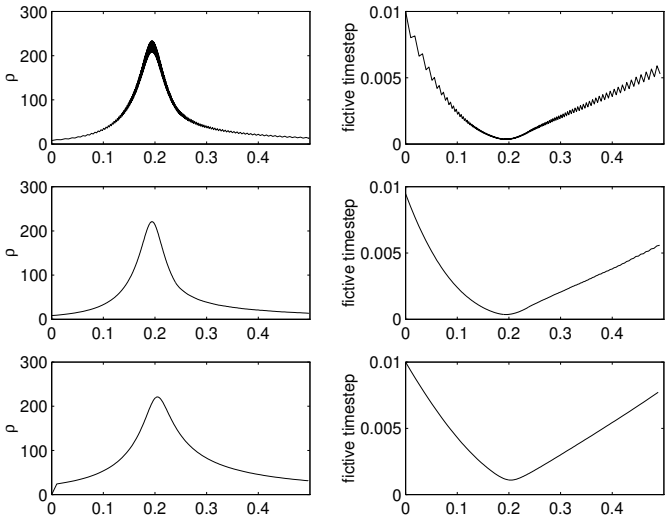

FIG. 9. *Time transformation variable* ρ *and size of fictive timestep for improperly initialized VRATTLE(A) (top views), correctly initialized VRATTLE(A) (middle views) with control function* U_3 *(eq. (5.52)). Bottom views give* ρ *and fictive timestep for VRATTLE(B) with function* $\tilde{U}_3$ *(eq. (6.53)) and* $\mu = \alpha = 3$*. In this case,* ρ *and the initial timestep are scaled by a constant for easier comparison.*

7. Conclusion. In this article we described a new variable stepsize approach for solving the constrained equations of motion which arise in the dynamics of molecular and mechanical systems. We presented several formulations for the time reparameterization function suitable for various situations in which occasional events in the dynamics require small timesteps for correct numerical resolution. Numerical experiments presented here show that VSHAKE/VRATTLE can eliminate large energy fluctuations associated with difficult regions in the dynamics, while increasing efficiency as compared to traditional fixed stepsize methods.

Although we have observed in our experiments that the stepsize wobble, a nonlinear artifact of explicit adaptive-reversible integration, can be ameliorated by proper initialization of the constraint equation, or eliminated by use of the implicit VRATTLE(B) method, we do not yet have a full understanding of its cause.

REFERENCES

[1] H.C. Andersen, *Rattle: a 'velocity' version of the shake algorithm for molecular dynamics calculations*, J. Comp. Phys., 52 (1983), pp. 24–34.

[2] S. Antman, *Nonlinear Problems of Elasticity*, Springer, New York, 1995.

[3] E. Barth, K. Kuczera, B. Leimkuhler and R.D. Skeel, *Algorithms for constrained molecular dynamics*, J. Comp. Chem., 16 (1995), pp. 1192–1209.

[4] E. Barth and B. Leimkuhler, *Symplectic methods for conservative multibody systems*, in Integration Algorithms for Classical Mechanics, Fields Institute Communications, vol. 10, American Mathematical Society, 1996, pp. 25–43.

[5] E. Barth, M. Mandziuk and T. Schlick, *A separating framework for increasing the timestep in molecular dynamics*, in Computer Simulation of Biomolecular Systems: Theoretical and Experimental Applications, Volume 3, W.F. van Gunsteren, P.K. Weiner and A. J. Wilkinson, Editors, ESCOM, Leiden, The Netherlands, 1996.

[6] D.G. Bettis and V. Szebehely, *Treatment of close approaches in the numerical integration of the gravitational problem of N bodies.* in Gravitational N-Body Problems, M. Lecar ed., D. Reidel Publishing Company, Dordrecht-Holland, 1972, pp. 388–405.

[7] M.P. Calvo and E. Hairer, *Accurate long term integration of dynamical systems*, Appl. Num. Math, 18 (1995), pp. 95–105.

[8] M.P. Calvo and J.M. Sanz-Serna, *Variable steps for symplectic integrators*, in Numerical Analysis 1991, D.F. Griffiths and G.A. Watson, Editors, Longman, London, pp. 34–48.

[9] D.J. Dichmann and J.H. Maddocks, *An impetus-striction simulation of the dynamics of an elastica*, J. Nonlinear Science, 6 (1996), pp. 271–292

[10] O. Gonzalez and J. Simo, *On the stability of symplectic and energy-momentum algorithms for Nonlinear Hamiltonian Systems with Symmetry*, Comp. Meth. Appl. Mech. Engr., 134 (1996), pp. 197–222.

[11] T. Hughes and J.E. Marsden, *Mathematical Foundations of Elasticity*, Prentice Hall, 1983, reprinted by Dover, 1994.

[12] E. Hairer, *Variable time step integration with symplectic methods*, preprint, 1996.

[13] P. Hut, J. Makino and S. Mcmillan, *Building a better leapfrog*, Astrophysical Journal Letters, 443 (1995), p. 93.

[14] W. Huang and B. Leimkuhler, *The Adaptive Verlet method*, SIAM J. Sci. Comp., vol. 18, number 1 (1997).

[15] B. Leimkuhler, S. Reich and R.D. Skeel *Integration methods for molecular dynamics*, in Mathematical Approaches to Biomolecular Structure and Dynamics, J. Mesirov, K. Schulten and D.W. Sumners eds., Springer IMA Series, vol. 82, 1996, pp. 161–186.

[16] B. Leimkuhler and R.D. Skeel, *Symplectic numerical integrators in constrained Hamiltonian systems*, J. Comp. Phys., 112 (1994), pp. 117–125.

[17] I. Klapper, *Biological applications of the dynamics of twisted rods*, Journal of Computational Physics, 125 (1996), pp. 325–337.

[18] M. Mandziuk and T. Schlick, *Resonance in chemical systems simulated by the implicit midpoint method*, Chem. Phys. Lett., 237 (1995), pp. 525–535.

[19] R.S. Manning, J.H. Maddocks and J.D. Kahn, *A continuum rod model of sequence-dependent DNA structure*, J. Chem. Phys., to appear October 1996.

[20] R.I. McLachlan and C. Scovel, *Equivariant constrained symplectic integration*, J. Nonlinear Science, 16 (1995), pp. 233–256.

[21] S. Reich, *Symplectic integrators for systems of rigid bodies*, in Integration Algorithms for Classical Mechanics, Fields Institute Communications, vol. 10, American Mathematical Society, 1996, pp. 181–191.

[22] S. Reich, *Backward error analysis for numerical integrators*, preprint, 1996.

[23] J.P. Ryckaert, G. Ciccotti and H.J.C. Berendsen, *Numerical integration of the Cartesian equations of motion of a system with constraints: molecular dynamics of n-alkanes*, J. Comp. Phys., 23 (1977), pp. 327–341.

[24] R.D. Skeel, *Variable step size destabilizes the Störmer/leap-frog/Verlet method*, BIT, 33 (1993), pp. 172–175.

[25] D.M. Stoffer, *Variable steps for reversible integration Methods*, Computing, 55 (1995), pp. 1–22.

[26] K.F. Sundman, *Memoire sur le probleme des trois corps*, Acta Math, 36 (1912), pp. 105–179.

[27] J.E. Marsden and J.M. Wendlandt, *Mechanical integrators with symmetry, variational principles, and integration algorithms*, in Proceedings of the Notre Dame Conference on New Directions in Applied Mathematics, Notre Dame, IN, to appear December, 1996.

[28] K. Zare and V. Szebehely, *Time transformations of the extended phase space*, Celestial Mechanics, 11 (1975), pp. 469–482.